



OPEN ACCESS

EDITED BY

Stavros Plessas,
Democritus University of Thrace, Greece

REVIEWED BY

Alejandra Romo-Araiza,
Anahuac University of North Mexico, Mexico
Anastasios Nikolaou,
Democritus University of Thrace, Greece

*CORRESPONDENCE

Kieran Rea
✉ kieran.rea@adm.com

†These authors have contributed equally to this work and share first authorship

SPECIALTY SECTION

This article was submitted to
Food Microbiology,
a section of the journal
Frontiers in Microbiology

RECEIVED 16 December 2022

ACCEPTED 13 March 2023

PUBLISHED 11 April 2023

CITATION

Simon A, Colom J, Mazhar S, Khokhlova E,
Deaton J and Rea K (2023) *Bacillus megaterium*
Renspore® as a potential probiotic for gut
health and detoxification of unwanted dietary
contaminants. *Front. Microbiol.* 14:1125616.
doi: 10.3389/fmicb.2023.1125616

COPYRIGHT

© 2023 Simon, Colom, Mazhar, Khokhlova,
Deaton and Rea. This is an open-access article
distributed under the terms of the [Creative Commons Attribution License \(CC BY\)](https://creativecommons.org/licenses/by/4.0/). The use,
distribution or reproduction in other forums is
permitted, provided the original author(s) and
the copyright owner(s) are credited and that
the original publication in this journal is cited, in
accordance with accepted academic practice.
No use, distribution or reproduction is
permitted which does not comply with these
terms.

Bacillus megaterium Renspore® as a potential probiotic for gut health and detoxification of unwanted dietary contaminants

Annie Simon^{1†}, Joan Colom^{1†}, Shahneela Mazhar^{1†},
Ekaterina Khokhlova^{1†}, John Deaton² and Kieran Rea^{1*}

¹ADM Cork H&W Ltd., Bioinnovation Unit, University College Cork, Cork, Ireland, ²Deerland Probiotics and Enzymes/ADM, Kennesaw, GA, United States

Exposure to diverse environmental pollutants and food contaminants is ever-increasing. The risks related to the bioaccumulation of such xenobiotics in the air and food chain have exerted negative effects on human health, such as inflammation, oxidative stress, DNA damage, gastrointestinal disorders, and chronic diseases. The use of probiotics is considered an economical and versatile tool for the detoxification of hazardous chemicals that are persistent in the environment and food chain, potentially for scavenging unwanted xenobiotics in the gut. In this study, *Bacillus megaterium* MIT411 (Renspore®) was characterized for general probiotic properties including antimicrobial activity, dietary metabolism, and antioxidant activity, and for the capacity to detoxify several environmental contaminants that can be found in the food chain. *In silico* studies revealed genes associated with carbohydrate, protein and lipid metabolism, xenobiotic chelation or degradation, and antioxidant properties. *Bacillus megaterium* MIT411 (Renspore®) demonstrated high levels of total antioxidant activities, in addition to antimicrobial activity against *Escherichia coli*, *Salmonella enterica*, *Staphylococcus aureus*, and *Campylobacter jejuni* *in vitro*. The metabolic analysis demonstrated strong enzymatic activity with a high release of amino acids and beneficial short-chain fatty acids (SCFAs). Moreover, Renspore® effectively chelated the heavy metals, mercury and lead, without negatively impacting the beneficial minerals, iron, magnesium, or calcium, and degraded the environmental contaminants, nitrite, ammonia, and 4-Chloro-2-nitrophenol. These findings suggest that Renspore® may play a beneficial role in supporting gut health metabolism and eliminating unwanted dietary contaminants.

KEYWORDS

probiotic, *Bacillus megaterium*, gut, microbiota

1. Introduction

While the rapid industrialization and urbanization of the last century have improved many facets of everyday life, there has been negative consequent contamination of soil and water resources which have impacted the food chain and human health (Zhao et al., 2005). Several pollutants that are highly toxic and difficult to degrade including heavy metals and xenobiotics such as flavorings, food additives, pesticides, and industrial chemicals are

detectable in water and food (Atashgahi et al., 2018; Feng et al., 2018; Srednicka et al., 2021). These environmental contaminants can negatively impact human and animal physiology affecting various organs and tissues and exacerbating undesirable symptoms including inflammation (Madani et al., 2015), oxidative stress (Nuran Ercal et al., 2005), and intestinal problems (Breton et al., 2013). As such, exclusion, degradation, or removal of these products from the food chain is of ever-increasing interest.

Several remedies have been developed to alleviate this phenomenon including the use of probiotics to protect against foodborne environmental contaminants (Feng et al., 2018). Probiotics are live microorganisms that benefit human health when supplemented in adequate amounts (Quigley, 2010). Probiotics possess health-promoting properties including antimicrobial activity, antioxidant and anti-inflammatory properties, immunomodulatory capacity, and production of bioactive molecules such as enzymes, short-chain fatty acids, and free amino acids among others (Minj et al., 2021). In addition, probiotic bacteria may possess intrinsic genetic machinery for eliminating environmental contaminants from the human body (Bisanz et al., 2014). Clinical research performed on pregnant women and children in Tanzania has suggested that probiotic yogurt can protect mothers and children from heavy metal poisoning (Bisanz et al., 2014). A review on the remediation of gut contaminants has also shown that *Lactobacilli* can alleviate toxicity caused by cadmium and decrease oxidative stress in cells (Feng et al., 2018). Among *Lactobacillus* species, *L. rhamnosus* GG is a widely researched probiotic strain that possesses most of the probiotic attributes, such as acid and bile resistance, adhesion ability, antimicrobial activity, antioxidant capacity, toxin removal ability, and heavy metal biosorption capability (Halttunen et al., 2008). *L. rhamnosus* GG has also been studied in the gut remediation of parathion pesticide and the degradation of aflatoxin from fungus (Feng et al., 2018; Westerik et al., 2018). Similarly, different spore probiotic species such as *B. subtilis*, *B. megaterium*, *B. coagulans*, and *B. pumilus* were also investigated for the removal of environmental contaminants using chelation or bioaccumulation principle (Elshaghabee et al., 2017). Interestingly, *Bacillus megaterium* has been studied for the elimination of environmental pollutants because of high levels of resistance to hostile conditions including exposure to heavy metals (Norma, 2018), with some strains demonstrating efficacy in the degradation of bisphenol A (BPA) present in industrial effluents, soil, and sludge (Suyamud et al., 2018).

In this study, we evaluated the probiotic properties of *B. megaterium* MIT411 (Renuspore[®]) and its impact on various aspects of host physiology, and the mechanisms involved in the bioremediation of environmental contaminants. For comparison, we used *L. rhamnosus* GG (ATCC 53103) or *L. fermentum* (obtained from a commercial product) as controls for our *in vitro* studies. We first interrogated the genomics of Renuspore[®] to identify specific genes, pathways, and enzymes that are responsible for the bioaccumulation or degradation of environmental contaminants and addressed their functional activity in the bioaccumulation of heavy metals and degradation of xenobiotics and finally investigated their mechanisms in bioremediation. In addition, *in silico* analysis of the enzymes involved in the proteolytic, lipolytic, and carbohydrate metabolism

pathways was performed, and a diverse enzymatic profile which includes protease activity, production of short-chain fatty acids (SCFA), and free amino acids (FAA) was demonstrated. These *in silico* findings were then tested with *in vitro* assays for antimicrobial, anti-inflammatory, antioxidant, and enzymatic capabilities to determine their potential as a therapeutic probiotic.

2. Materials and methods

2.1. Bacterial strains

Renuspore[®], a spore-forming, Gram-positive, rod-shaped bacteria, was obtained from Deerland Probiotics and Enzymes/ADM, Kennesaw, USA. Renuspore[®] was subjected to 16S DNA sequencing by Eurofins genomics, Germany. NCBI GenBank and BLAST tools were used to confirm the sequences and species. Indicator strains, namely *Escherichia coli* 25922, *Salmonella enteritidis* 13076, *Pseudomonas aeruginosa* DSM3227, *Staphylococcus aureus* RF122, and *Campylobacter jejuni* DSM4688, were sourced from Deutsche Sammlung von Mikroorganismen und Zellkulturen (DSMZ), Germany. Comparator probiotic strain such as *Lactobacillus rhamnosus* GG was purchased from an American type cell culture collection (ATCC 53103), while *Lactobacillus fermentum* was isolated from a commercially available product. All strains, except for *L. fermentum*, were grown aerobically in tryptic soy broth (TSB) medium at 37°C for 18 h at 170 RPM. *L. fermentum* was grown under the same conditions using MRS broth. For counts, all strains were plated on tryptic soy agar (TSA) medium. The vegetative form of Renuspore[®] (1×10^8 CFU/ml) was used in all *in vitro* studies. In addition, spores of Renuspore[®] (1×10^8 CFU/ml) were used in the adhesion ability assay. All media were purchased from Sigma-Aldrich, Ireland Ltd.

2.2. Genomic analysis

The genes encoding antioxidants, heavy metals, nitrite degradation, and proteolytic, lipolytic, and carbohydrate metabolism pathways were analyzed from the genome sequence data, which were retrieved from NCBI GenBank (NZ_JABBNK010000001). The complete GenBank file was used in RAST subsystem technology to find and annotate protein-encoding genes (Jyoti et al., 2022). All the genes involved in protein and lipid metabolism were screened to facilitate comparison with metabolomic and enzymatic data. Each gene was cross-referenced with the Renuspore[®] genome file for confirmation.

2.3. Antimicrobial activity

The antimicrobial activity of Renuspore[®] (*B. megaterium* MIT411) was tested using the agar diffusion method (Balouiri et al., 2016). A measure of 10 μ L of cultured Renuspore[®] at 1×10^8 CFU/mL concentration was inoculated at the center of the TSA agar plate, air-dried, and incubated at 37°C for 18 h. Post-incubation, the Renuspore[®] spotted agar plates were overlaid with 5 mL of fresh molten TSA agar (0.4%) inoculated with 100-fold dilutions of

cultured pathogen strains. The plates were incubated at 37°C for 24 h, and the zones of inhibition were recorded in mm. Control strains were not indicated in the assay as the antimicrobial activity was performed to establish probiotic property of Renuspire®.

2.4. Antioxidant and reduced glutathione activity

The total antioxidant capacity and reduced glutathione (GSH) activity of Renuspire® and *L. rhamnosus* GG were quantified by colorimetric analysis at 570 nm and 420 nm, respectively, using the total antioxidant capacity (TAC) (MAK187, Sigma-Aldrich, Ireland) (Ibrahim et al., 2021) and Reduced Glutathione Assay Kits (E-BC-K030-S, Elabscience, China). For these studies, both strains were grown in the TSB medium at 37°C until a final concentration of 1×10^8 CFU/mL was reached. The culture was then centrifuged at 6,000 RPM for 15 min, and the supernatant was discarded. The cell pellet was washed and resuspended in 1X PBS three times. The washed cell pellet was resuspended in 1.5 mL 1X PBS and homogenized three times at 3,500 RPM for 30 s using a microtube homogenizer (Beadbug, Benchmark, Ireland). The homogenized sample was centrifuged at 6,000 RPM for 15 min at 4°C. The cell debris was discarded, and the cell lysate was recovered for testing. 1X PBS was used as a negative control. The TAC and reduced glutathione assay were performed following the manufacturer's instructions.

2.5. Adhesion study

HT-29 (a human colorectal adenocarcinoma cell line) and mucous-secreting cell line HT-29-MTX (ATCC), purchased from ATCC, were routinely maintained in DMEM low glucose medium supplemented with 10% fetal bovine serum, 1% L-glutamine, and antimicrobials such as penicillin (100 U/mL) and streptomycin (100 µg/mL). Cell lines were incubated in a 5% CO₂ atmosphere at 37°C. Cells were seeded onto 24-well plates at a density of 5×10^5 cell/well and cultured for 21–28 days to complete maturation.

Before the experiment, cells were washed two times with 0.5 mL DPBS, and 0.4 mL of full media without antibiotics was added to each well. Bacterial cells were added to the cell lines, and the adhesion ability was determined by bacterial cell counts in CFU/mL.

Since the adhesion ability of *L. fermentum* has been well-established and also has two times higher adhesion capacity to *L. rhamnosus* GG in HT-29 cell lines (Gharbi et al., 2019), bacterial adhesion capacity to HT-29 and HT-29 MTX cell lines was investigated in Renuspire® and *L. fermentum*. Renuspire® (vegetative and spores) and *L. fermentum* with a final concentration of 10^8 CFU/mL and 10^7 CFU/mL, respectively, were added to the cell lines. The bacterial suspension and cell lines were incubated for 3.5 h at 37°C in a humidified atmosphere at 5% CO₂. Controls were prepared in a similar way without the cell lines. Bacterial adherence ability was assessed at 37°C. After incubation, the cell layers were washed four times with DPBS to remove non-adherent bacteria, before the cell layers were detached by the addition of

Trypsin/EDTA (Sigma-Aldrich, USA) (Letourneau et al., 2011; Gagnon et al., 2013; Tsilia et al., 2015). The remaining suspensions with viable adhered bacteria were diluted and plated onto TSA or MRS agar. The number of colony-forming units was counted after aerobic incubation at 37°C for 24 h.

2.6. Heavy metal bioaccumulation

2.6.1. Mercury and lead

Renuspire® and *L. rhamnosus* GG were cultured aerobically in TSB medium (Sigma-Aldrich, Ireland Ltd.) supplemented with 1 ppm of lead or mercury (Sigma-Aldrich, Ireland Ltd.) until they reached a final concentration of 1×10^8 CFU/mL. Cultures were centrifuged at 6,000 RPM for 15 min at room temperature, and the supernatants were saved. TSB medium supplemented with 1 ppm lead or mercury was set as control. Saved supernatants and controls were filter-sterilized and sent to Eurofins Food Testing Ireland Limited for quantification by ICP-MS analysis. ICP-MS (Agilent 7900) consists of plasma, a mass spectrometer with a quadrupole mass filter, and a detector. All liquids were converted to aerosol by pumping into the nebulizer. The saved supernatants and control samples were carried in a gas stream of plasma in the form of an aerosol. The high-temperature electrical discharge of plasma transformed samples into vapors to atomize and ionize the elements. The ionized particles were then separated, and the analyte ions were filtered by the quadrupole mass filter. The filtered mass was finally counted by the detector (González-Antuña et al., 2017).

2.6.2. Iron, calcium, and magnesium bioaccumulation

Renuspire® and *L. rhamnosus* GG were cultured aerobically in TSB medium (Sigma-Aldrich, Ireland Ltd.) supplemented with 500 µM of calcium and 10 ppm of iron or magnesium (Sigma-Aldrich, Ireland Ltd.), until they reached a final concentration of 10^8 CFU/mL. Cultures were centrifuged at 6,000 RPM for 15 min at room temperature, and the supernatants were saved. TSB medium supplemented with 500 µM of calcium and 10 ppm of iron or magnesium was set as control. Saved supernatants and controls were filter-sterilized and analyzed using an Iron Assay Kit (Sigma-Aldrich, MAK025, Ireland Ltd.), Calcium Assay Kit (Cell Biolabs, MET5121, USA), and Magnesium Microplate Assay Kit (Cohesion biosciences, CAK1107), according to the manufacturer's instructions.

2.7. Xenobiotic degradation

2.7.1. Nitrite detoxification

Renuspire® and *L. rhamnosus* GG were cultured in TSB supplemented with 100 µM nitrite solution (Sigma-Aldrich, 72586, Ireland Ltd.) until they reached 10^8 CFU/mL. Cultures were centrifuged at 6,000 RPM for 15 min at room temperature, and the supernatants were saved. TSB medium with 100 µM nitrite solution

was set as control. The saved supernatants and control were filter-sterilized and analyzed using a Nitrite/Nitrate Assay Kit (Sigma-Aldrich, 23479, Ireland Ltd.). The levels of nitrite were measured at 570 nm, following the manufacturer's instructions.

2.7.2. Ammonia degradation

To evaluate the growth and ability of Rensuore[®] to metabolize ammonia, Rensuore[®] and *L. rhamnosus* GG were inoculated in supplemented minimal media which contained ammonium chloride. Minimal media were supplemented with 2% of 1M glucose, 0.2% of 1M magnesium sulfate, and 0.01% of 1M calcium chloride. The inoculated media were incubated at 37°C for 24 h at 170 RPM. The supplemented minimal media without any strain were set as control. Ammonia or ammonium present in the filter-sterilized control and supernatants of Rensuore[®] and *L. rhamnosus* GG were measured at 620 nm using an Ammonia/Ammonium Assay Kit (Abbeva, abx298905, UK) following the manufacturer's instructions.

2.7.3. 4-Chloro-2-nitrophenol (4C2NP) degradation

Rensuore[®] (1×10^8 CFU/mL) was cultured for 24 h in minimal media containing 10 mM glucose, 0.20 % of 1M magnesium sulfate, 0.01% of 1M calcium chloride, and various concentrations of the xenobiotic 4-Chloro-2-nitrophenol (0.25, 0.5, 1.0, 1.5 and 2.0 mM) dissolved in ethyl alcohol. Every 2 h, 2 mL of samples were collected and centrifuged at 6,000 RPM for 15 min to observe 4C2NP decolorization in the supernatant. The 4C2NP decolorization was measured with the decrease in the optical density at 405 nm, and the percentage of decolorization was calculated as described by Arora (2012) using the following calculation:

$$\% \text{ Decolorization} = (\text{Initial Absorbance} - \text{Absorbance after time } t) \times 100 / \text{Initial Absorbance}.$$

Control strain was not indicated in the assay since *L. rhamnosus* GG was unable to grow in the presence of 4C2NP in the supplemented minimal media.

2.8. Carbohydrate fermentation

To evaluate carbohydrate metabolism in Rensuore[®], API 50 CH, a standardized system, comprising 49 biochemical tests, was used. Several pure identical single colonies of Rensuore[®] were picked and suspended in an ampule of API NaCl 0.85% medium (Biomérieux, Ref 70700) until turbidity was equivalent to 2 McFarland (Biomérieux, Ref 70900). The prepared suspension was transferred to an ampule of API 50 CHB/E medium (Biomérieux, Ref 50430). Two hundred microliters of the inoculated API 50 CHB/E medium were added into the strip wells and incubated for 48 h. A positive test corresponded to acidification revealed by the phenol red indicator contained in the medium changing to a yellow color. Control strain was not indicated in the assay since carbohydrate fermentation was performed to analyze the potential probiotic properties of Rensuore[®].

2.9. Enzymatic activity

The enzymatic profiling was performed by API ZYM (API Laboratory Products Ltd., Biomérieux, France), a semi-quantitative method, comprising 19 naphthyl substrates to evaluate the enzymatic activities of Rensuore[®]. Several pure identical single colonies of Rensuore[®] were picked and suspended in an ampule of API suspension medium (Biomérieux, Ref 70700) until turbidity was equivalent to 6 McFarland (Biomérieux, Ref 70900). Two hundred microliters of the inoculated API suspension medium were added into the strip wells and incubated for 48 h. Post-incubation, the reactions were read on the color chart according to the manufacturer's manual. Control strain was not indicated as the assay was performed to determine the enzymatic activity of the probiotic Rensuore[®].

2.10. Protease activity

The quantitative extracellular protease activity in the solution was investigated in Rensuore[®] by employing a commercial EnzChek[®] Protease Assay Kit (Molecular Probes, Eugene, OR, USA), which contains a casein derivative labeled with green-fluorescent BODIPY[®] FL dye.

The cells of Rensuore[®] and *L. rhamnosus* GG (1×10^8 CFU/mL) were washed and suspended in 100 µl of 1X PBS for the assay. Proteinase K was used as a positive control, and all samples were assayed with an incubation time of 24 h using the EnzChek[®] Protease Assay Kit, according to the manufacturer's instructions. Fluorescence (Ex/ Em 485/ 535 nm) was measured on a Tecan Microplate Reader using standard filters.

2.11. Free amino acids (FAAs) and short-chain fatty acids (SCFAs)

Rensuore[®] (1×10^8 CFU/mL) was cultured in ultra-high-temperature (UHT) milk (Indomilk, Semarang, Central Java, Indonesia). The culture was incubated at 37 °C for 48 h with shaking. A cell-free supernatant was used to analyze FAA and SCFA. Control strain was not tested for FAA and SCFA since the objective of the assay was to investigate the metabolites of Rensuore[®]. The uninoculated UHT milk was used as a negative control. MS-Omics (Vedbæk, Denmark) performed mass spectrometry to analyze FAA and SCFA. Hydrochloride acid was used to acidify the sample, and deuterium-labeled internal standards were used for analysis. All samples were analyzed by GC (7890B, Agilent), combined with a quadrupole detector (5977B, Agilent) where a high polarity column (Zebron[™] ZB-FFAP, GC Cap. Column 30 m × 0.25 mm × 0.25 µm) was installed. All raw data were formatted to net CDF via Chemstation (Agilent). The final data were imported and assessed in Matlab R2014b (Mathworks Inc.) through PARADISE software (Johnsen et al., 2017).

2.12. Statistical analysis

Degradation of the 4-Chloro-2-nitrophenol (4C2NP) data was analyzed using a two-way analysis of variance (ANOVA), followed by Dunnett's multiple comparison test. The free amino acid and short-chain fatty acid GC-MS results were analyzed using multiple *t*-tests using unpaired parametric, two-stage step-up (Benjamini, Krieger, and Yekutieli). All other results were statistically analyzed using the one-way analysis of variance (ANOVA) (biological replicates $n = 3$ or 5), followed by Tukey's multiple comparison test using GraphPad Prism v.9.

3. Results

3.1. Genomic analysis

Whole-genome sequencing analysis showed Renuspire[®] genome is composed of 5,429,269 base pairs with no plasmids (using classic RAST annotations), and it encodes 5,429 coding genes and 171 RNA genes. Genes involved in the antioxidant activity (*Cu/Zn-SOD*, *Mn-SOD*, *Fe-SOD*, *Ni-SOD*, *CAT*, *GPx*,

PRDX, *TXN*, *TXNRD*, and *NIR*) and heavy metal sequestration (*mer* and *ars*) have been associated with the *in vitro* total antioxidant capacity assay and ICP-MS heavy metal detection, respectively. In addition, genes linked to proteolytic activity and FAA and SCFA production were also observed. The number of possible genes encoding enzymes and transporters involved in carbohydrate metabolism and enzymatic activity was identified during genomic analysis. To correlate the genomic findings, the API 50 CH strips were employed for *in vitro* investigation. In carbohydrate fermentation, more than two genes were identified in the breakdown of D-ribose (*rbsA*, *rbsB*, *rbsD*, *rpiA*, and *rpiB*), D-xylose (*xylA*, *xylE*, and *xylB*), D-glucose (*Gdh*, *galT*, *galU*, *G6PD*, and *GlcU*), and D-trehalose (*treR*, *treB*, *thuA*, and *treA*). Although Renuspire[®] API 50CH results indicated positive fermentation of D-saccharose, D-maltose, D-melezitose, D-raffinose, amidon, glycogen, D-sorbitol, N-acetylglucosamine, and esculin ferric citrate (Table 1), the genes related to the metabolism of these carbohydrates were not identified in Renuspire[®] genome (Table 1). Similarly, the API 50 CH identification kit was used to confirm the genomic findings of Renuspire[®]'s enzymatic profiling which included esterase activity (*EstA*, *fes*, *lpqC*, *paal*, and *fadM*,

TABLE 1 Renuspire[®] can ferment 11 carbohydrates using API 50 CH strips, and the genes associated with the fermentation were indicated from the genomic analysis.

Carbohydrates	-/+	Possible genes	Carbohydrates	-/+	Possible genes
L-arabinose	+	<i>AraA</i> , <i>araD</i>	Salicin	-	
D-ribose	+	<i>rbsA</i> , <i>rbsB</i> , <i>rbsD</i> , <i>rpiA</i> , <i>rpiB</i>	D-cellobiose	-	
D-xylose	+	<i>xylA</i> , <i>xylE</i> , <i>xylB</i>	Inulin	-	
D-mannitol	+	<i>mtlD</i>	D-lactose	-	<i>Ldh</i> , <i>lutP</i>
D-glucose	+	<i>Gdh</i> , <i>galT</i> , <i>galU</i> , <i>G6PD</i> , <i>GlcU</i>	D-melibiose	-	
D-fructose	+	<i>pfkA</i> , <i>fsaA</i>	Glycerol	-	
D-trehalose	(+)	<i>treR</i> , <i>treB</i> , <i>thuA</i> , <i>treA</i>	Erythritol	-	
D-saccharose	+		D-arabinose	-	
D-maltose	+		Methyl-Ad-mannopyranoside	-	
D-melezitose	(+)		Xylitol	-	
D-rafinose	(+)		Gentiobiose	-	
Amidon	(+)		D-turanose	-	
Glycogen	(+)		D-Lyxose	-	
D-sorbitol	+		D-tagatose	-	
N-acetylglucosamine	+		D-fucose	-	
Esculin ferric citrate	+		L-fucose	-	
L-xylose	-		Methyl-Bd-xylopyranoside	-	
D-adonitol	-		D-galactose	-	<i>galB</i> , <i>galA</i>
L-sorbose	-		D-mannose	-	
L-rhamnose	-		Pottasium 5-ketogluconate	-	
Dulcitol	-		Arbutin	-	
Inositol	-	<i>idh</i>	D-arabitol	-	
Methyl-Ad-glucopyranoside	-		L-arabitol	-	
Pottasium 2-ketogluconate	-		Pottasium gluconate	-	
Amygdalin	-				

Legends indicate the following: +, positive; -, negative; (+), weakly positive.

TABLE 2 Semi-quantitative assay of enzyme activities of Renuspo[®] using API ZYM kit (n = 3), where + indicates the presence and—indicates the absence of enzymes.

Function	Possible genes	Enzymes	+/-
Esterase activity	<i>EstA, fes, lpqC, paal, fadM</i>	Esterase (C4:0)	+
		Esterase (C8:0)	+
Lipase activity	<i>tesA</i>	Lipase (C14:0)	-
Peptidase activity	<i>oppA, oppF, DppB, DppD, DppC, pcp, Map, pepB, pepP, pepX, pepE, pepF, pepV, pepD</i>	Leucine arylamidase	-
		Valine arylamidase	-
		Cystine arylamidase	-
Proteinase activity		Trypsin	-
		α -chymotrypsin	+
Phosphatase activity		Acid phosphatase	-
		Alkaline phosphatase	+
		Phosphohydrolyase	+
Glycosidase activity	<i>galA</i>	α -Galactosidase	+
	<i>galB</i>	β -Galactosidase	+
		β -Glucuronidase	-
		α -Glucosidase	-
		β -Glucosidase	-
		β -Glucosaminidase	-
		α -Mannosidase	-
		α -Fucosidase	-

lipase activity (*tesA*), peptidase activity (*oppA, oppF, DppB, DppD, DppC, pcp, Map, pepB, pepP, pepX, pepE, pepF, pepV, and pepD*), and glycosidase activity (*galA and galB*) (Table 2). Although the genomic analysis revealed genes for carbohydrate, protein, and lipid metabolism, the *in vitro* studies did not fully correlate with the genes identified.

3.2. Antimicrobial activity

A total of five opportunistic and zoonotic pathogens of the gut, the urinary tract, and the skin were selected for evaluating the antimicrobial properties of Renuspo[®]. Renuspo[®] had an antimicrobial activity with a hazy zone of inhibition observed against *E. coli*, *S. enteritidis*, *S. aureus*, and *C. jejuni* on the TSA overlaid with 0.4% TSA agar (Table 3). No antimicrobial activity was observed against *P. aeruginosa*.

3.3. Antioxidant and reduced glutathione activity

From the genomic analysis, genes encoding antioxidant enzymes were identified in Renuspo[®]. Antioxidant genes such as superoxide dismutase (Cu/Zn-SOD, Mn-SOD, Fe-SOD, and Ni-SOD), catalase (CAT), glutathione peroxidase (GPx), peroxiredoxin (PRDX), thioredoxin (TXN), thioredoxin reductase (TXNRD), and nitrite reductase (NIR) were detected in Renuspo[®]. The genomic data were correlated with the *in vitro* models compared with *L. rhamnosus* GG. In *in vitro* antioxidant capacity and reduced glutathione activity assays, Renuspo[®] (1×10^8 CFU/mL) demonstrated superior antioxidant capacity [Figure 1, $F_{(2,6)} = 98.13$, $p < 0.0001$] and increased mgGSH [Figure 1, $F_{(2,6)} = 443.7$, $p < 0.0001$] output as compared with a known antioxidant probiotic *L. rhamnosus* GG.

TABLE 3 Renuspo[®] had moderate antimicrobial activity against *E. coli*, *S. enteritidis*, *S. aureus*, and *C. jejuni* in solid media (TSA).

Renuspo [®]	Zone of inhibition (mm)				
	<i>E. coli</i>	<i>S. enteritidis</i>	<i>S. aureus</i>	<i>C. jejuni</i>	<i>P. aeruginosa</i>
	18.9 ± 0.9	18.7 ± 1.2	18.67 ± 0.58	21.1 ± 1.44	No inhibition

Antimicrobial activity is indicated as zone of inhibition (mm) ± standard deviation. The results were statistically analyzed by the Student's t-test analysis (biological replicates n=3) using GraphPad Prism v.9.

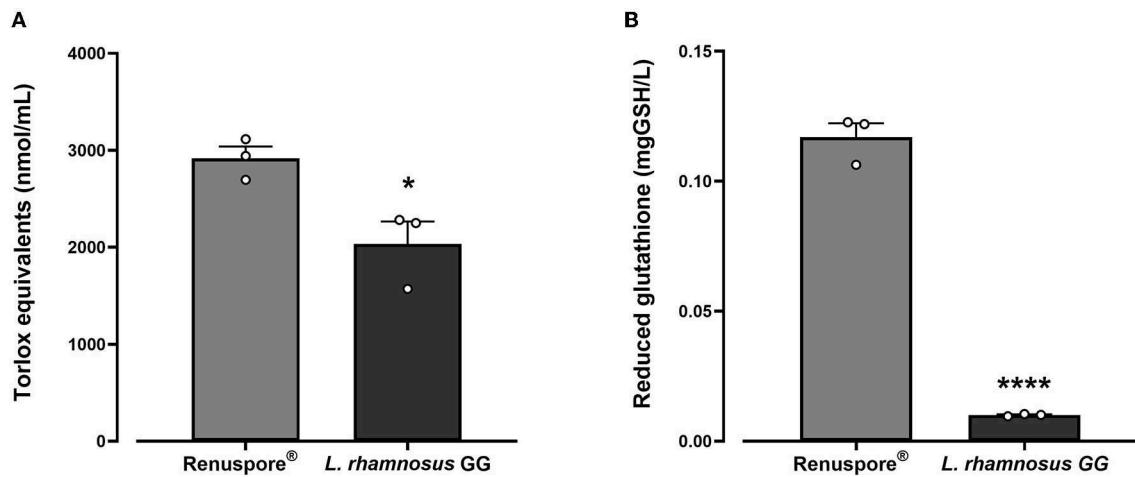


FIGURE 1

Renuspoire® had significantly increased levels of (A) Trolox equivalents and (B) reduced glutathione GSH compared with *L. rhamnosus* GG. The results show average concentration ($n = 3$) \pm standard error. Significant difference observed between Renuspoire® and *L. rhamnosus* GG: * $p < 0.05$ and **** $p < 0.0001$. The results were statistically analyzed using one-way analysis of variance (ANOVA) (biological replicates $n = 3$) followed by Tukey's multiple comparison test using GraphPad Prism v.9.

3.4. Adhesion study

The adhesion ability of Renuspoire® and *L. fermentum* (control) was studied in human colorectal adenocarcinoma cell lines HT-29 and HT-29-MTX at 37°C. Renuspoire® vegetative cells do not adhere to the HT-29 and HT-29 MTX

at 37°C, whereas at 37°C, the spores of *B. megaterium* MIT411 adhered to the intestinal cell lines HT-29 [Figure 2A, $F_{(2,13)} = 81.60$, $p < 0.0001$] and mucus-producing HT-29 MTX cell lines [Figure 2B, $F_{(2,15)} = 99.52$, $p < 0.0001$]. *B. megaterium* MIT411 spores had low adhesion ability compared with *L. fermentum*.

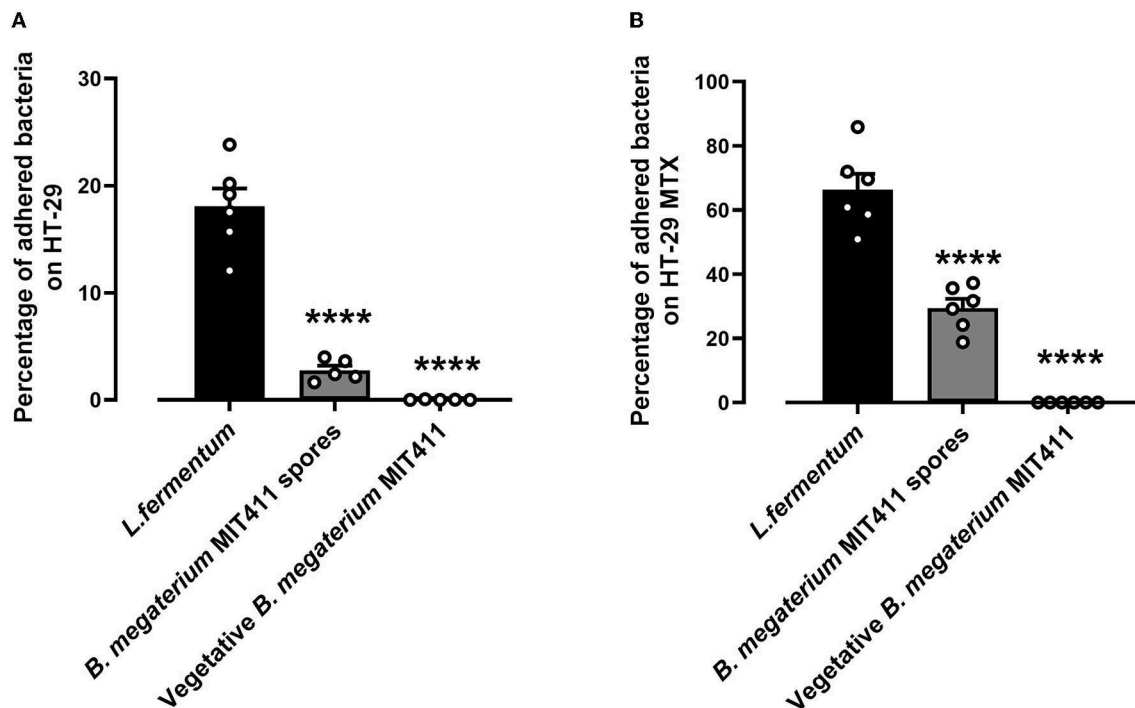


FIGURE 2

Renuspoire® does not significantly adhere to (A) HT-29 and (B) HT-29 MTX cells at 37°C compared with *L. fermentum*. Significant difference observed between Renuspoire® and *L. fermentum*. **** $p < 0.0001$. The results were statistically analyzed using Student's t -test analysis (biological replicates $n = 6$) using GraphPad Prism v.9.

3.5. Heavy metal bioaccumulation

When exposed to some of the most common toxic heavy metals in the environment, Renuspore[®] effectively bioaccumulated lead [Figure 3A, $F_{(2,17)} = 10.71$, $p < 0.001$] and mercury [Figure 3B, $F_{(2,17)} = 77.02$, $p < 0.0001$] compared with control and probiotic

strain *L. rhamnosus* GG. From Figure 3, in the presence of essential metals and minerals, Renuspore[®] does not bioaccumulate iron [Figure 3C, $F_{(2,6)} = 0.4633$, $p > 0.5$], calcium [Figure 3D, $F_{(2,6)} = 2.017$, $p < 0.5$], and magnesium [Figure 3E, $F_{(2,9)} = 2.736$, $p < 0.5$], thereby not compromising natural absorption of essential minerals in the body.

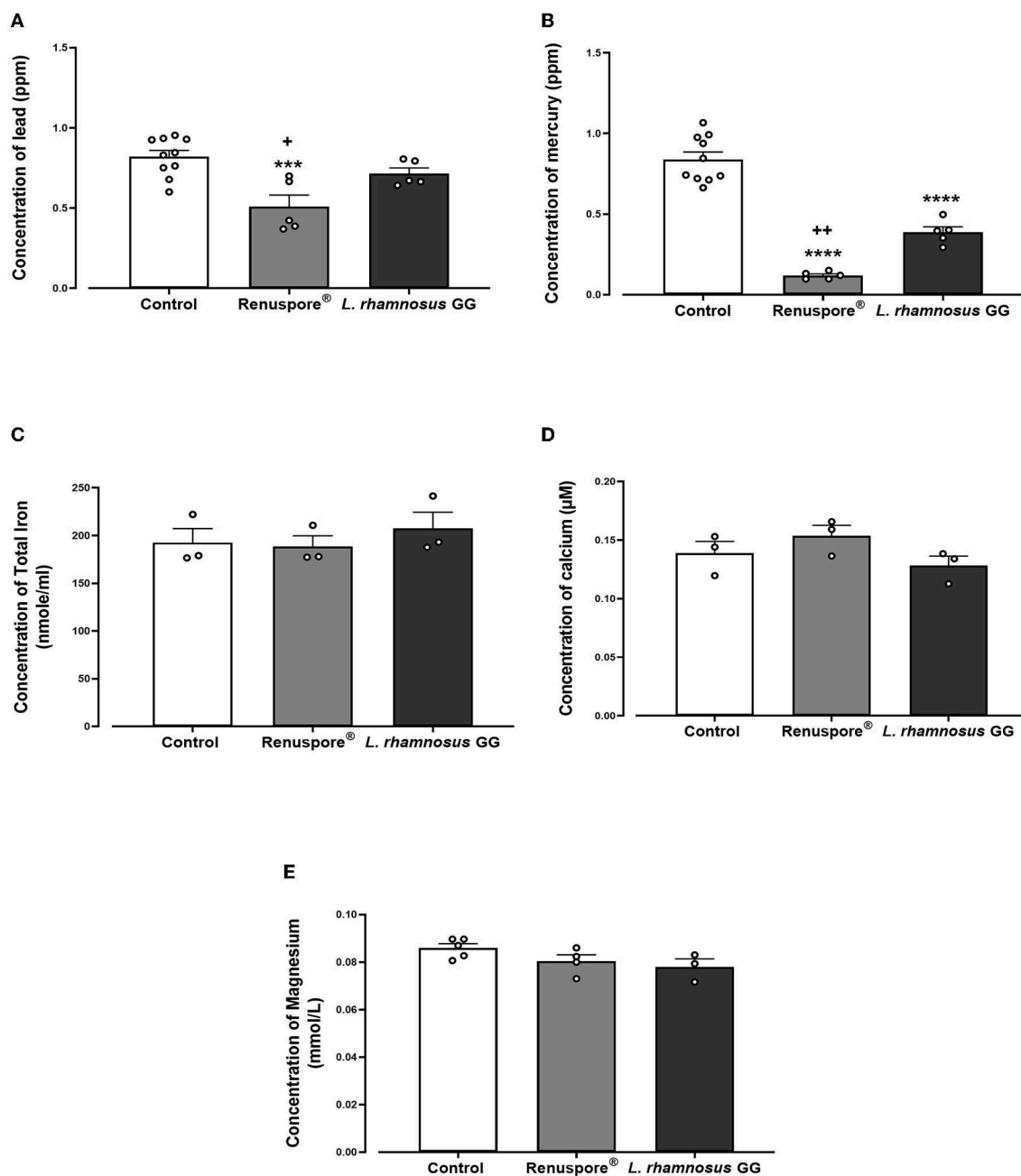


FIGURE 3

Renuspore[®] significantly decreased the concentration of (A) lead and (B) mercury compared with *L. rhamnosus* GG. The results show average concentration ($n = 5$) \pm standard error. Renuspore[®] does not bioaccumulate (C) iron, (D) calcium, and (E) magnesium. The results show average concentration ($n = 3$) \pm standard error. Significant difference observed between Renuspore[®] and control is indicated: *** $p < 0.001$ and **** $p < 0.0001$. Significant reduction observed between Renuspore[®] and *L. rhamnosus* GG is indicated: + $p < 0.05$ and ++ $p < 0.01$. The results were statistically analyzed using the one-way analysis of variance (ANOVA) (biological replicates $n = 3$ or 5) followed by Tukey's multiple comparison test using GraphPad Prism v.9.

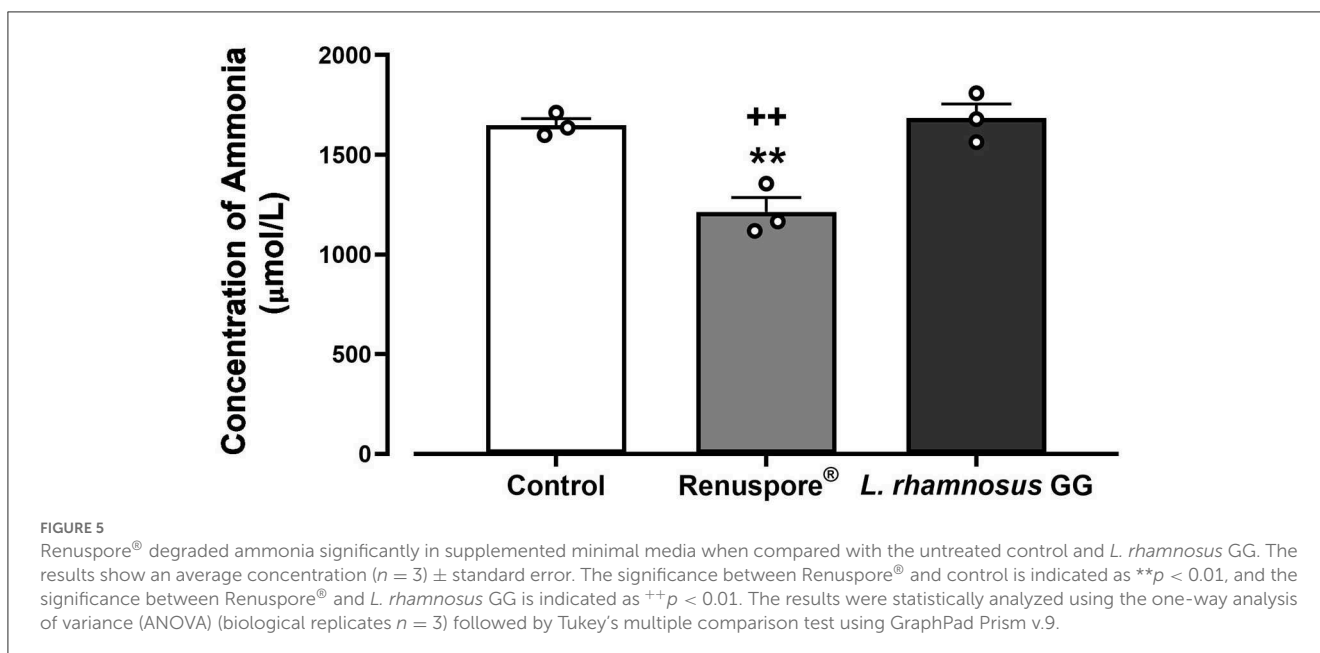
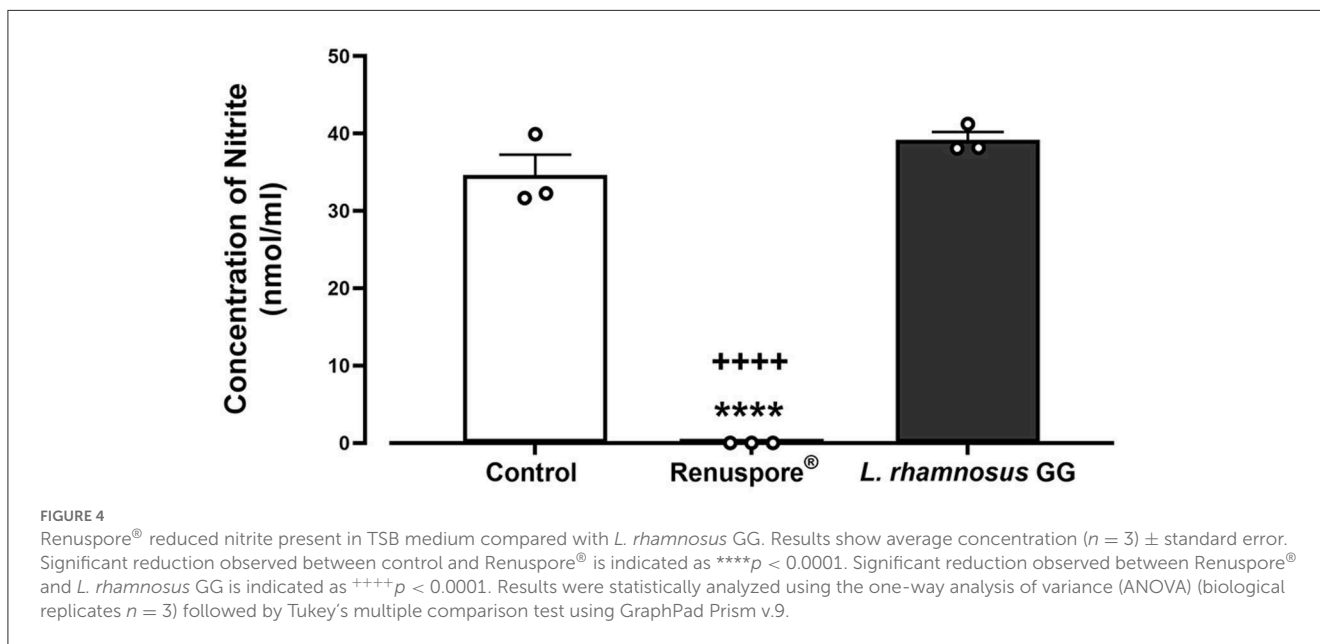
3.6. Xenobiotic degradation

3.6.1. Nitrite detoxification

A genomic analysis of Renspore[®] reveals the presence of genes encoding the enzyme nitrite reductase (*NirD*), which conventionally reduces nitrite to ammonium (Yukioka et al., 2017). In this study, *in vitro* analysis demonstrated the ability of Renspore[®] to reduce nitrite present in TSB medium below the limit of detection, whereas *L. rhamnosus* GG did not alter the concentration [Figure 4, $F_{(2,6)} = 168.9, p < 0.0001$].

3.6.2. Ammonia degradation

To test for the ability of Renspore[®] to degrade ammonia from the environment, Renspore[®] and the control strain *L. rhamnosus* GG were cultured in minimal media supplemented with ammonium chloride as the sole nitrogen source. Renspore[®] significantly decreased ammonia levels when compared with *L. rhamnosus* GG as determined by the Ammonia/Ammonium Assay Kit (Abbexa, UK) measured at 620 nm [Figure 5, $F_{(2,6)} = 18.10, p < 0.01$].



3.6.3. 4-Chloro-2-nitrophenol (4C2NP) degradation

Renuspore[®] decolorized 4C2NP up to 0.5 mM concentration proving the degradation of the xenobiotic [Figure 6, $F_{(12,52)} = 19.96$, $p < 0.0001$]. Renuspore[®] rapidly decolorized at 0.25 mM concentration of 4C2NP in 10–16 h of incubation. At 0.5 mM concentration, Renuspore[®] degraded 4C2NP in 18–24 h. Renuspore[®] showed a limited decolorization at 1–1.5 mM concentration, and no decolorization at the concentration of 2.0 mM as Renuspore[®] was unable to grow in these conditions (Figure 6).

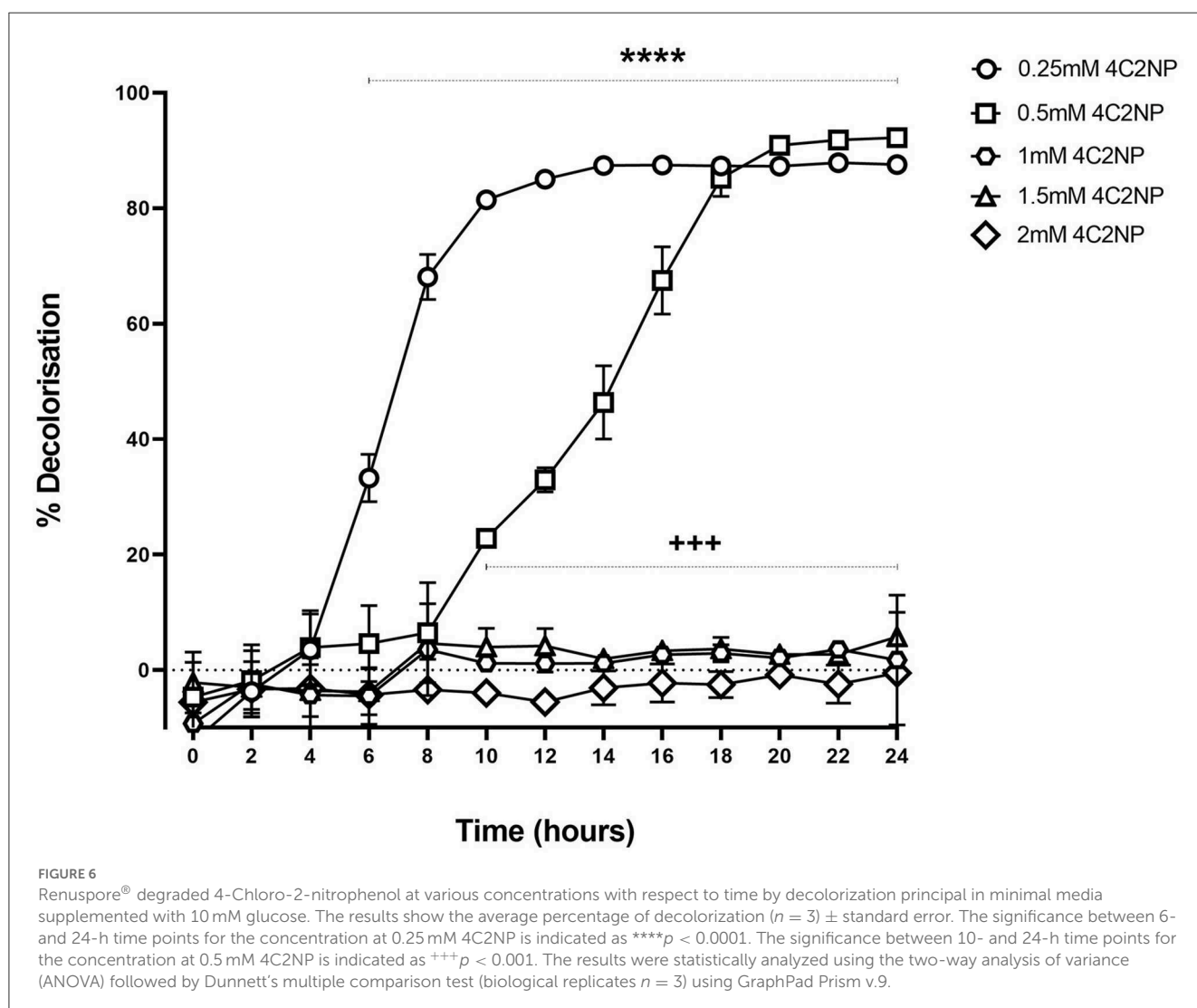
3.7. Carbohydrate fermentation

Renuspore[®] has the ability to ferment 11 carbohydrates out of the 49 tested carbohydrates using a commercial API 50 CH strip (Table 1). The *in vitro* analysis was confirmed with the genomic analysis and their possible genes encoding carbohydrate metabolism.

In silico analysis in the genome of Renuspore[®] reported the presence of transporters and enzymes involved in the metabolism of D-ribose, L-arabinose, D-xylose, D-glucose, D-fructose, and D-mannitol, whereas enzymes for D-maltose, N-acetylglucosamine, D-saccharose, and D-sorbitol were not identified. In addition, genes involved in the metabolism of trehalose, lactose, galactose, inositol, and amylase A (*amyA*) involved in starch metabolism were also identified in the genome of Renuspore[®]; however, the results of the API test did not directly correlate with the presence of these genes.

3.8. Proteolytic activity

Genomic analysis data show genes encoding protease activity in Renuspore[®] include *clpC*, *clpP*, *clpX*, and *prp*. The assay determining the protease activity is based on the principle that the measured increase in fluorescence at Ex/Em 485/535 nm is proportional to the proteinase activity. Renuspore[®] showed a significant amount of extracellular protease activity when



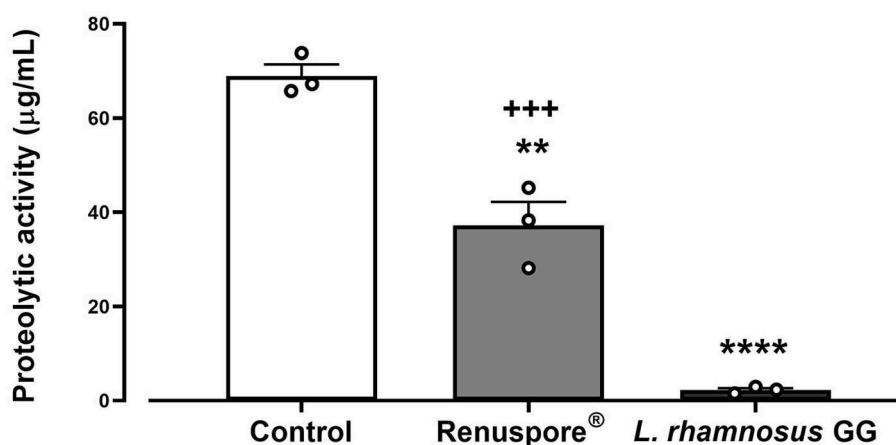


FIGURE 7

Renuspire® demonstrates superior protease activity ($\mu\text{g}/\text{mL}$) to *L. rhamnosus* GG. The results show average concentration ($n = 3$) \pm standard error. Significant difference observed between Renuspire® and positive control (Proteinase K): $**p < 0.01$. Significant difference observed between Renuspire® and *L. rhamnosus* GG: $+++p < 0.001$. The results were statistically analyzed using the one-way analysis of variance (ANOVA) (biological replicates $n = 3$) followed by Tukey's multiple comparison test using GraphPad Prism v.9. Significant difference observed between *L. rhamnosus* GG and control (Proteinase K) is indicated: $****p < 0.0001$.

compared with *L. rhamnosus* GG [Figure 7, $F_{(2,6)} = 108.1$, $p < 0.0001$].

3.9. Enzymatic profiling

Renuspire® showed a range of peptidase, esterase, phosphatase, proteinase, lipase, and glycosidase activities (Table 2). Renuspire® was characterized by strong esterase, α -chymotrypsin, alkaline phosphatase, phosphohydrolase, α -galactosidase, and β -galactosidase activities. From *in silico* analysis, genes encoding β -galactosidase, α -galactosidase, esterase, and peptidase were also identified although this did not directly correlate with the *in vitro* test results.

3.10. Free amino acids (FAAs) and short-chain fatty acids (SCFAs)

A metabolomic analysis revealed the proteolytic capability of Renuspire® toward milk proteins generating a diverse range of amino acids. Out of 44 compounds, 30 were found to be statistically significant in Renuspire® (Table 4, $p < 0.05$).

TABLE 4 Renuspire® increased FAA in UHT fermented milk compared with the control (uninoculated UHT milk): $*p \leq 0.05$.

Compound	p -value	$t_{(df)} = t$ ratio
Alanine	0.0142	$t_{(4)} = 4.158$
glycine	0.2862	$t_{(4)} = 1.230$
Valine	0.0000	$t_{(4)} = 22.01$
Leucine	0.0002	$t_{(4)} = 12.84$

(Continued)

TABLE 4 (Continued)

Compound	p -value	$t_{(df)} = t$ ratio
Isoleucine	0.0001	$t_{(4)} = 16.65$
Threonine	0.0105	$t_{(4)} = 4.545$
Proline	0.0096	$t_{(4)} = 4.658$
Aspartic acid	0.0153	$t_{(4)} = 4.067$
Glutamic acid	0.0170	$t_{(3)} = 4.817$
Methionine	0.0009	$t_{(4)} = 8.979$
Phenylalanine	0.0027	$t_{(4)} = 6.622$
Lysine	0.0002	$t_{(3)} = 21.34$
Histidine	0.0295	$t_{(3)} = 3.922$
Tyrosine	0.0005	$t_{(4)} = 10.43$
Tryptophan	0.0012	$t_{(4)} = 8.126$
Cystine	0.0132	$t_{(4)} = 4.243$
Ornithine	< 0.000001	$t_{(3)} = 153.0$
Serine	0.0024	$t_{(4)} = 6.871$
Fumaric acid	0.0173	$t_{(4)} = 3.917$
4-Aminobenzoic acid	0.1161	$t_{(4)} = 2.000$
Succinic acid	0.0065	$t_{(4)} = 5.205$
Lactic acid	> 0.9999	
2-Oxoglutaric acid	0.0003	$t_{(3)} = 19.67$
2-Phosphoenolpyruvic acid	0.0048	$t_{(3)} = 7.584$
Malic acid	0.0198	$t_{(4)} = 3.760$
cis-Aconitic acid	0.0002	$t_{(4)} = 13.73$
Citric acid	0.0000	$t_{(4)} = 45.11$

(Continued)

TABLE 4 (Continued)

Compound	p-value	$t_{(df)} = t$ ratio
Isocitric acid	0.0001	$t_{(4)} = 15.05$
Alanyl-proline	0.0023	$t_{(3)} = 9.774$
Glycyl-proline	0.0008	$t_{(3)} = 14.06$
Octanoic acid	0.0647	$t_{(4)} = 2.529$
5-Aminovaleric acid	0.0000	$t_{(4)} = 21.78$
Benzoic acid	0.0000	$t_{(4)} = 23.73$
Phenylacetic acid	0.0005	$t_{(3)} = 15.85$
Decanoic acid	0.2097	$t_{(4)} = 1.493$
Decenoic acid	0.0211	$t_{(4)} = 3.684$
N-Acetyl-valine	0.0005	$t_{(4)} = 10.13$
Dodecanoic acid	0.1342	$t_{(4)} = 1.874$
Tetradecanoic acid	0.3271	$t_{(4)} = 1.115$
3-(methylthio)propionic acid	0.0001	$t_{(3)} = 25.67$
Pyruvic acid	0.0014	$t_{(3)} = 11.54$
4-methyl-2-oxopentanoic acid	0.0111	$t_{(3)} = 5.623$
3-Methyl-oxirane-2-carboxylic acid	0.0078	$t_{(3)} = 6.368$
4-Hydroxyphenylacetic acid	0.0014	$t_{(3)} = 11.42$

The results were statistically analyzed using multiple t-tests using the unpaired parametric, two-stage step-up (Benjamini, Krieger, and Yekutieli) (biological replicates $n = 3$) using GraphPad Prism v.9.

TABLE 5 SCFA increased in Renuspor® UHT-fermented milk samples: * $p \leq 0.05$.

Compound	p-value	$t_{(df)} = t$ ratio
Acetic acid	0.0114	$t_{(4)} = 4.433$
Formic acid	0.2552	$t_{(4)} = 1.327$
Propionate	0.0003	$t_{(4)} = 12.23$
2-methyl- propionate	0.0001	$t_{(4)} = 17.23$
Butyrate	0.3387	$t_{(4)} = 1.086$
3-methyl-butyrate	0.0791	$t_{(4)} = 2.344$
4-methyl-pentanoic acid	0.7519	$t_{(4)} = 0.3386$
Hexanoic acid	0.7670	$t_{(4)} = 0.3171$
Heptanoic acid	0.3340	$t_{(4)} = 1.098$

The results were statistically analyzed using multiple t-test using unpaired parametric, two-stage step-up (Benjamini, Krieger, and Yekutieli) (biological replicates $n = 3$) using GraphPad Prism v.9.

A genomic analysis revealed the presence of oligopeptide (*Opp*) and dipeptide (*DtpP*) transporters, which are involved in the proteolysis of peptides to FAA by the action of peptidases. Aminopeptidases and metallopeptidases which are responsible for generating methionine and leucine or their derivatives were identified in the Renuspor® genome. Proline peptidase (*pepP* and *pepX*), endopeptidase (*pepE* and *pepF*), and dipeptidase (*pepV* and *pepD*) were also found in the Renuspor® genome.

For the SCFA analysis, a total of nine compounds were identified, of which only three were found to be significantly increased by Renuspor® (Table 5). Interestingly, these were acetic

acid, propionate, and 2-methyl-propionate. Propionate is usually associated with amino acid metabolism, specifically alanine and valine (Tavaria et al., 2002). A few esterases and lipases potentially related to the metabolic pathways of these SCFAs were identified in Renuspor®'s genome. Esterase A (*estA*), which shows relatively high activity toward β -naphthyl butyrate, and tannase/feruloyl esterase, which hydrolyzes bonds of tannic acid, feruloyl-arabinose ester bond in arabinoxylans, as well as the feruloyl-galactose and feruloyl-arabinose ester bonds in pectin, were identified. Lipase (*tesA*) belongs to class 3, which has been reported to hydrolyze long-chain acyl-triglycerides into di- and monoglycerides, glycerol, and free fatty acids (Cadwallader and Singh, 2009).

4. Discussion

In this study, the general probiotic properties of Renuspor® were characterized. A common property shared by many probiotic strains is the capacity to inhibit the growth of pathogens and positively impact the gut microbial composition by producing antimicrobial agents or metabolic compounds that suppress the growth of other microorganisms (O'Shea et al., 2012). Renuspor® had antimicrobial activity against both Gram-negative and Gram-positive bacteria, with the capacity to control zoonotic, opportunistic intestinal, skin, and urinary tract pathogens such as *Salmonella*, *E. coli*, *S. aureus*, and *C. jejuni*. Probiotic secondary metabolites can act as strong antimicrobial agents against pathogens and can also indirectly boost the host's defenses by modulating the host's immune or epithelial cells (Machado et al., 2021). Although classic antimicrobial compounds such as bacteriocins or lantibiotics produced by *Bacillus* species (Caulier et al., 2019) were not detected in Renuspor®'s genome, *in vitro* results suggest that it can inhibit the growth of several pathogens. Recent studies demonstrated how propionate and acetic acid had bactericidal activity against MRSA, *E. coli*, *Salmonella typhimurium*, and *C. albicans* independently of pH changes (Wali and Abed, 2019; Langfeld et al., 2021). Therefore, it is possible that high levels of acetic acid and propionate produced by Renuspor® could be the reason for the antimicrobial activity observed in this study. It is essential for a probiotic in human nutrition to modulate metabolite production (Markowiak-Kope and Sli, 2020). An *In vitro* study made in UHT milk demonstrated significant levels of propionate production (Table 5). Consequently, Renuspor® ingestion may increase propionate production in the gut and promote its anti-inflammatory properties and help lower lipogenesis and cholesterol levels in serum (Hosseini et al., 2011). Propionate production was likely linked to Renuspor® esterolytic activity, with genes encoding esterase A and lipases.

Renuspor® also demonstrated strong proteolytic activity against proteins present in milk, generating 30 free amino acids and carboxylic acids. The 30 free amino acid compounds increased in this *in vitro* test are a direct result of protease and peptidase activities. With its high proteolytic activity, Renuspor®'s presence in the gut could increase levels of FAA, which in turn would help regulate digestion, support the immune system, enhance mucous integrity and function, or act as an energy source for the human body (Kim et al., 2019). The phenotypic findings involved in the metabolism and transport of carbohydrates, proteins, and lipids

do not always affiliate with specific genes. The *in vitro* studies in Renspore[®] did not completely infer the presence and absence of the associated genes. The disparity between the genome and *in vitro* analysis could be due to gene variations and additional protein-dependent sugar uptake systems with overlapping substrate or host conditions adaptability (Kilic et al., 2007; Buron-Moles et al., 2019). There are genes encoding enzymes identified as involved in trehalose, lactose, and inositol metabolism, whereas our investigation using API 50 CH indicated Renspore[®]'s weak ability to ferment trehalose with no fermentation achieved for lactose or inositol. The reason for this disagreement could be that the set of genes involved in the uptake and metabolism of these sugars are incomplete, or these were false negatives and should be confirmed with a conventional phenol red broth or other more sensitive methods. In contrast, with other properties of many probiotics, Renspore[®] vegetative cells were unable to adhere to the intestinal cells or their secreted mucous, although they showed moderate adherence in their spore form. Therefore, in the intestinal tract, the spore form could adhere and germinate to vegetative cells, which would offer their potential probiotic effects. Since the vegetative form has a low adherence capacity, it is possible that Renspore[®] would be able to sequester heavy metals from the gut and then be washed out, helping remove these elements from the intestine.

In addition, beneficial bacterial metabolites and enzymes can influence the metabolism of xenobiotics and reactive oxygen species directly or indirectly by regulating the expression and function of key antioxidant liver enzymes (Clarke et al., 2019). Environmental contaminants such as heavy metals, nitrite, ammonia, and pesticides enter the food chain and can cause oxidative stress to the body. Oxidative stress then leads to cell death, and ingestion of these toxic heavy metals can cause multiorgan failure and immune system suppression (Syed and Chinthala, 2015). Probiotics have been known to offer protection against reactive oxygen species and oxidative stress and to be able to scavenge these molecules. *Lactobacillus* species have been reported to have antioxidant properties that work against heavy metal-induced oxidative stress in mice (Srednicka et al., 2021). Renspore[®] has been shown to have high levels of antioxidant molecules and glutathione compared with *L. rhamnosus* GG (Figure 1). These results correlated with the presence of antioxidant enzymes encoded in the Renspore[®] genome, suggesting that this probiotic strain could offer oxidative stress protection in the gut, shield cellular macromolecules from reactive oxygen and nitrogen species, and directly neutralize oxidative chemicals (Demirkol and Ercal, 2014). All these findings on Renspore[®] could possibly prevent leaky gut, intestinal disorders, cell damage, and diseases caused by reactive oxidative species imbalance in the body.

Since pollutants such as heavy metals are ubiquitous and unavoidable, various strategies including microbial bioremediation are being researched and implemented for the treatment and prevention of toxin exposures (Bisanz et al., 2014). Probiotic detoxification mechanisms include either sequestration to the bacterial cell wall or biosorption of metal ions into the bacterial cell wall which is followed by bioaccumulation within the bacterial cell through cell membrane transition (Abdel-Megeed, 2021). Several studies reported that *Lactobacillus* and *Saccharomyces* species have the potential to eliminate heavy metals either by binding or by biosorption (Bhakta et al., 2012; Alcántara et al., 2017; Duan et al., 2020). Similarly, *in vitro* studies showed the capacity of

Renspore[®] to remove lead and mercury from the environment (Figure 3). This capacity to remove non-essential heavy metals could be related to the presence of *mer* and *ars* operons in the Renspore[®] genome (Giovannella et al., 2016), which encode proteins involved in mercury or lead regulation, binding, or degradation (Boyd and Barkay, 2012). Moreover, since Gram-positive bacteria have higher metal-binding activity, the affinity mechanism in Renspore[®] can act as a physical barrier in the gut to modify the absorption and metabolism of heavy metals (Abdel-Megeed, 2021). In addition, higher levels of glutathione production by Renspore[®] can support the transportation of mercury out of cells, facilitates the excretion of organic and toxic metal pollutants from the body, and can directly neutralize oxidative chemicals (Demirkol and Ercal, 2014).

Considering the xenobiotic contamination in the food chain, ammonia and nitrites are commonly present in the waste from poultry and aquaculture which can pollute soil and water ecosystem including the shrimps and fishes that humans consume (Anwar et al., 2021). In addition, ammonia and nitrites present in meat and cheese in the form of additives and flavoring can be toxic to human health (Karwowska and Kononiuk, 2020). Most bacterial species rely on xenobiotics for energy sources, and they have particular genes, enzymes, and degradative mechanisms to partially or completely metabolize xenobiotics. *B. subtilis* species were used to maintain (Zokaeifar et al., 2014) and decrease the concentrations of ammonia, nitrite, and nitrate levels in laying hens (Mi et al., 2019). The presence of a gene encoding the enzyme nitrite reductase, *NirD*, could explain how Renspore[®] was able to reduce and degrade nitrite (Hou et al., 2013) from the environment. Finally, microbial degradation has proven to be effective at degrading contaminants from industrial effluents such as chloronitrophenol (Arora, 2012). Data from the 4-Chloro-2-nitrophenol (4C2NP) decolorization result show the degradation capacity of Renspore[®] with respect to time (Figure 6). A study from the genomics and transcriptomics on *Rhodococcus* species suggests that 4-nitrophenol breaks down into acetyl-coA and succinate by nitrocatechol through *Nph*-specific genes (Migliani et al., 2022), facilitating the further metabolism of this hazardous pesticide. All these endocrine disruptors that are present in the environmental chemicals may contribute to the ecosocionomic burden by increasing human diseases and disabilities (Kassotis et al., 2020). Consumption of the probiotic strain Renspore[®] could potentially facilitate effective detoxification of such undesirable metabolites and reduced accumulation of environmental contaminants, thus reducing biological and physiological complications.

5. Conclusion

Globally, there is an unmet need for products to help cleanse and detoxify environmental contaminants in the food and water supply chains. Applications for microbes in the bioremediation of environmental contaminants represent a viable solution. More specifically, on an individual level, the role of probiotics in the removal of unwanted intrinsic and extrinsic toxins from the body is a very desirable trait. Renspore[®] may act as a catalyst in enhancing the natural biodegradation or sequestration of xenobiotics from our gut, and/or chelating and removing heavy metals by ion exchange, adsorption, or metal-binding proteins.

Renuspire[®] can also break down the desired pollutant through various enzymatic pathways and biochemical reactions. This xenobiotic bioreduction capacity of Renuspire[®] represents natural technology to protect our health from contaminants present in the food chain. The *in silico* and *in vitro* data presented herein demonstrate the antimicrobial, antioxidant, and bioremediation properties of Renuspire[®]. Further beneficial probiotic effects include strong enzymatic activity against proteins, lipids, and carbohydrates to assist in food digestion, and the generation of various biomolecules known to be important in nutrient absorption. In summary, these findings suggest that Renuspire[®] represents a strong probiotic candidate for facilitating gut and overall body health.

Data availability statement

Publicly available datasets were analyzed in this study. This data can be found here: NCBI GenBank (NZ_JABBNK010000001) https://www.ncbi.nlm.nih.gov/nucleotide/NZ_JABBNK010000001.

Author contributions

AS, SM, EK, and JC performed the sample analysis. JD and KR were the advisor for the study and reviewed the manuscript.

References

- Abdel-Megeed, R. M. (2021). Probiotics: a promising generation of heavy metal detoxification. *Biol. Trace Elem. Res.* 199, 2406–2413. doi: 10.1007/s12011-020-02350-1
- Alcántara, C., Jadán-Piedra, C., Vélez, D., Devesa, V., Zúñiga, M., and Monedero, V. (2017). Characterization of the binding capacity of mercurial species in *Lactobacillus* strains. *J. Sci. Food Agric.* 97, 5107–5113. doi: 10.1002/jsfa.8388
- Anwar, K., Safitri, R., Fajriani, N., Gifari, Z. A., Wariata, I. W., Rosyidi, A., et al. (2021). In Vitro screening of ammonia and nitrite-degrading bacteria isolated from broiler chicken (*Gallus gallus domesticus*) intestines and pond sediment of Nile tilapia (*Oreochromis niloticus*): a preliminary study. *IOP Conf. Ser. Earth Environ. Sci.* 913, 012072. doi: 10.1088/1755-1315/913/1/012072
- Arora, P. K. (2012). Decolourization of 4-chloro-2-nitrophenol by a soil bacterium, *Bacillus subtilis* RKJ 700. *PLoS ONE* 7, e52012. doi: 10.1371/journal.pone.0052012
- Atashgahi, S., Shetty, S. A., Smidt, H., and de Vos, W. M. (2018). Flux, impact, and fate of halogenated xenobiotic compounds in the gut. *Front. Physiol.* 9, 888. doi: 10.3389/fphys.2018.00888
- Balouiri, M., Sadiki, M., and Ibsouda, S. K. (2016). Methods for *in vitro* evaluating antimicrobial activity: a review. *J. Pharm. Anal.* 6, 71–79. doi: 10.1016/j.jpha.2015.11.005
- Bhakta, J. N., Ohnishi, K., Muneke, Y., Iwasaki, K., and Wei, M. Q. (2012). Characterization of lactic acid bacteria-based probiotics as potential heavy metal sorbents. *J. Appl. Microbiol.* 112, 1193–206. doi: 10.1111/j.1365-2672.2012.05284.x
- Bisanz, J. E., Enos, M. K., Mwanga, J. R., Changalucha, J., Burton, J. P., Gloor, G. B., et al. (2014). Randomized open-label pilot study of the influence of probiotics and the gut microbiome on toxic metal levels in Tanzanian pregnant women and school children. *mBio*. 5, e01580–14. doi: 10.1128/mBio.01580-14
- Boyd, E. S., and Barkay, T. (2012). The mercury resistance operon: from an origin in a geothermal environment to an efficient detoxification machine. *Front. Microbiol.* 3, 349. doi: 10.3389/fmicb.2012.00349
- Breton, J., Massart, S., Vandamme, P., De Brandt, E., Pot, B., and Foligné, B. (2013). Ecotoxicology inside the gut: impact of heavy metals on the mouse microbiome. *BMC Pharmacol. Toxicol.* 14, 62. doi: 10.1186/2050-6511-14-62
- Buron-Moles, G., Chailyan, A., Dolejs, I., Forster, J., and Mikš, M. H. (2019). Uncovering carbohydrate metabolism through a genotype-phenotype association

AS contributed to the writing of the manuscript. All authors contributed to the article and approved the submitted version.

Funding

This study received funding from Deerland Probiotics and Enzymes. The funder was not involved in the study design, collection, analysis, interpretation of data, writing of this article, or the decision to submit it for publication.

Conflict of interest

AS, JC, SM, EK, and KR were employed by ADM Cork H&W Ltd. JD was employed by Deerland Probiotics and Enzymes.

Publisher's note

All claims expressed in this article are solely those of the authors and do not necessarily represent those of their affiliated organizations, or those of the publisher, the editors and the reviewers. Any product that may be evaluated in this article, or claim that may be made by its manufacturer, is not guaranteed or endorsed by the publisher.

study of 56 lactic acid bacteria genomes. *Appl. Microbiol. Biotechnol.* 103, 3135. doi: 10.1007/s00253-019-09701-6

Cadwallader, K. R., and Singh, T. K. (2009). Flavours and off-flavours in milk and dairy products. *Adv. Dairy Chem.* 3, 631–690. doi: 10.1007/978-0-387-84865-5_14

Caulier, S., Nannan, C., Gillis, A., Licciardi, F., Bragard, C., and Mahillon, J. (2019). Overview of the antimicrobial compounds produced by members of the *Bacillus subtilis* group. *Front. Microbiol.* 10, 302. doi: 10.3389/fmicb.2019.00302

Clarke, G., Sandhu, K. V., Griffin, B. T., Dinan, T. G., Cryan, J. F., and Hyland, N. P. (2019). Gut reactions: breaking down xenobiotic-microbiome interactions. *Pharmacol. Rev.* 71, 198–224. doi: 10.1124/pr.118.015768

Demirkol, O., and Ercal, N. (2014). Glutathione! *Integrative Med. Clinicians J.* 13, 8. doi: 10.1201/b11653

Duan, H., Yu, L., Tian, F., Zhai, Q., Fan, L., and Chen, W. (2020). Gut microbiota: a target for heavy metal toxicity and a probiotic protective strategy. *Sci. Total Environ.* 742, 140429. doi: 10.1016/j.scitotenv.2020.140429

Elshaghabe, F. M. F., Rokana, N., Gulhane, R. D., Sharma, C., and Panwar, H. (2017). *Bacillus* as potential probiotics: Status, concerns, and future perspectives. *Front. Microbiol.* 8, 1490. doi: 10.3389/fmicb.2017.01490

Feng, P., Ye, Z., Kakade, A., Virk, A. K., Li, X., and Liu, P. (2018). A review on gut remediation of selected environmental contaminants: possible roles of probiotics and gut microbiota. *Nutrients* 11, 22. doi: 10.3390/nu11010022

Gagnon, M., Zihler Berner, A., Chervet, N., Chassard, C., and Lacroix, C. (2013). Comparison of the Caco-2, HT-29 and the mucus-secreting HT29-MTX intestinal cell models to investigate *Salmonella* adhesion and invasion. *J. Microbiol. Methods* 94, 274–279. doi: 10.1016/j.mimet.2013.06.027

Gharbi, Y., Fhoula, I., Ruas-Madiedo, P., Afef, N., Boudabous, A., Gueimonde, M., et al. (2019). In-vitro characterization of potentially probiotic *Lactobacillus* strains isolated from human microbiota: interaction with pathogenic bacteria and the enteric cell line HT29. *Ann. Microbiol.* 69, 61–72. doi: 10.1007/s13213-018-1396-1

Giovanella, P., Cabral, L., Bento, F. M., Gianello, C., and Camargo, F. A. O. (2016). Mercury (II) removal by resistant bacterial isolates and mercuric (II) reductase activity in a new strain of *Pseudomonas* sp. B50A. *New Biotechnol.* 33, 216–223. doi: 10.1016/j.nbt.2015.05.006

- González-Antuña, A., Camacho, M., Henríquez-Hernández, L. A., Boada, L. D., Almeida-González, M., Zumbado, M., et al. (2017). Simultaneous quantification of 49 elements associated to e-waste in human blood by ICP-MS for routine analysis. *MethodsX*. 4, 328–334. doi: 10.1016/j.mex.2017.10.001
- Halttunen, T., Collado, M. C., El-Nezami, H., Meriluoto, J., and Salminen, S. (2008). Combining strains of lactic acid bacteria may reduce their toxin and heavy metal removal efficiency from aqueous solution. *Lett. Appl. Microbiol.* 46, 160–165. doi: 10.1111/j.1472-765X.2007.02276.x
- Hosseini, E., Grootaert, C., Verstraete, W., and Van de Wiele, T. (2011). Propionate as a health-promoting microbial metabolite in the human gut. *Nutr. Rev.* 69, 245–258. doi: 10.1111/j.1753-4887.2011.00388.x
- Hou, J., Cao, X., Song, C., and Zhou, Y. (2013). Predominance of ammonia-oxidizing archaea and nirK-gene-bearing denitrifiers among ammonia-oxidizing and denitrifying populations in sediments of a large urban eutrophic lake (Lake Donghu). *Can. J. Microbiol.* 59, 456–464. doi: 10.1139/cjm-2013-0083
- Ibrahim, D., Moustafa, A., Shahin, S. E., Sherief, W. R. I. A., Abdallah, K., Farag, M. F. M., et al. (2021). Impact of fermented or enzymatically fermented dried olive pomace on growth, expression of digestive enzyme and glucose transporter genes, oxidative stability of frozen meat, and economic efficiency of broiler chickens. *Front. Vet. Sci.* 8, 644325. doi: 10.3389/fvets.2021.644325
- Johnsen, L. G., Skou, P. B., Khakimov, B., and Bro, R. (2017). Gas chromatography - mass spectrometry data processing made easy. *J. Chromatograph. A.* 1503, 57–64. doi: 10.1016/J.CHROMA.2017.04.052
- Jyoti, C., Saini, S., Kumar, V., Abrol, K., Pandey, K., and Sharma, A. (2022). *Comparative Analysis of Gene Prediction Tools: RAST, Genmark hmm and AMIgene*. Available online at: <http://www.ijettjournal.org> (accessed March 25, 2022).
- Karwowska, M., and Kononiuk, A. (2020). Nitrates/nitrites in food-risk for nitrosative stress and benefits. *Antioxidants* 9, 241. doi: 10.3390/antiox9030241
- Kassotis, C. D., Vandenberg, L. N., Demeneix, B. A., Porta, M., Slama, R., and Trasande, L. (2020). Endocrine-disrupting chemicals: economic, regulatory, and policy implications. *Lancet Diabetes Endocrinol.* 8, 719. doi: 10.1016/S2213-8587(20)30128-5
- Kilic, A. O., Honeyman, A. L., and Tao, L. (2007). Overlapping substrate specificity for sucrose and maltose of two binding protein-dependent sugar uptake systems in *Streptococcus mutans*. *FEMS Microbiol. Lett.* 266, 218–223. doi: 10.1111/j.1574-6968.2006.00522.x
- Kim, S. W., Bradford, B., Blachier, F., Liao, S. F., and Yang, Z. (2019). Physiological effects of dietary amino acids on gut health and functions of swine. *Front. Vet. Sci.* 6, 169. doi: 10.3389/fvets.2019.00169
- Langfeld, L. Q., Du, K., Bereswill, S., and Heimesaat, M. M. (2021). A review of the antimicrobial and immune-modulatory properties of the gut microbiota-derived short chain fatty acid propionate – what is new? *Eur. J. Microbiol. Immunol.* 11, 50. doi: 10.1556/1886.2021.00005
- Letourneau, J., Levesque, C., Berthiaume, F., Jacques, M., and Mourez, M. (2011). *In vitro* assay of bacterial adhesion onto mammalian epithelial cells. *J. Vis. Exp.* 51, 51. doi: 10.3791/2783
- Machado, M. G., Sencio, V., and Trottein, F. (2021). Short-chain fatty acids as a potential treatment for infections: a closer look at the lungs. *Infect. Immun.* 89, e0018821. doi: 10.1128/IAI.00188-21
- Madani, F. Z., Hafida, M., Merzouk, S. A., Loukidi, B., Taouli, K., and Narce, M. (2015). Hemostatic, inflammatory, and oxidative markers in pesticide user farmers. *Biomarkers* 21, 138–145. doi: 10.3109/1354750X.2015.1118545
- Markowiak-Kope, P., and Sli, K. (2020). The effect of probiotics on the production of short-chain fatty acids by human intestinal microbiome. *Nutrients* 12, 1107. doi: 10.3390/nu12041107
- Mi, J., Chen, X., and Liao, X. (2019). Screening of single or combined administration of 9 probiotics to reduce ammonia emissions from laying hens. *Poult. Sci.* 98, 3977–3988. doi: 10.3382/ps/pez138
- Migliani, R., Parveen, N., Kumar, A., Ansari, M. A., Khanna, S., Rawat, G., et al. (2022). Degradation of xenobiotic pollutants: an environmentally sustainable approach. *Metabolites* 12, 818. doi: 10.3390/metabo12090818
- Minj, J., Chandra, P., Paul, C., and Sharma, R. K. (2021). Bio-functional properties of probiotic *Lactobacillus*: current applications and research perspectives. *Crit. Rev. Food Sci. Nutr.* 61, 2207–2224. doi: 10.1080/10408398.2020.1774496
- Norma, G. R.-A. (2018). Study of *Bacillus megaterium* potential application for high metal content residues biotreatment. *Open J. Bacteriol.* 4–8. doi: 10.17352/ojb.000007
- Nuran Erçal, B. S. P., Hande Gurer-Orhan, B. S. P., and Nukhet Aykin-Burns, B. S. P. (2005). Toxic metals and oxidative stress part I: mechanisms involved in metal induced oxidative damage. *Curr. Top. Med. Chem.* 1, 529–539. doi: 10.2174/1568026013394831
- O'Shea, E. F., Cotter, P. D., Stanton, C., Ross, R. P., and Hill, C. (2012). Production of bioactive substances by intestinal bacteria as a basis for explaining probiotic mechanisms: bacteriocins and conjugated linoleic acid. *Int. J. Food Microbiol.* 152, 189–205. doi: 10.1016/j.ijfoodmicro.2011.05.025
- Quigley, E. M. M. (2010). Prebiotics and probiotics; modifying and mining the microbiota. *Pharmacol. Res.* 61, 213–218. doi: 10.1016/j.phrs.2010.01.004
- Srednicka, P., Juszczak-Kubiak, E., Wójcicki, M., Akimowicz, M., and Roszko, M. (2021). Probiotics as a biological detoxification tool of food chemical contamination: a review. *Food Chem. Toxicol.* 153, 112306. doi: 10.1016/j.fct.2021.112306
- Suyamud, B., Inthorn, D., Panyapinyopol, B., and Thiravetyan, P. (2018). Biodegradation of bisphenol A by a newly isolated *Bacillus megaterium* strain iso-2 from a polycarbonate industrial wastewater. *Water Air Soil Pollut.* 229, 1–12. doi: 10.1007/s11270-018-3983-y
- Syed, S., and Chinthala, P. (2015). Heavy metal detoxification by different bacillus species isolated from solar salterns. *Scientifica* 2015, 1–8. doi: 10.1155/2015/319760
- Tavaria, F. K., Dahl, S., Carballo, F. J., and Malcata, F. X. (2002). Amino acid catabolism and generation of volatiles by lactic acid bacteria. *J. Dairy Sci.* 85, 2462–2470. doi: 10.3168/jds.S0022-0302(02)74328-2
- Tsilia, V., Van den Abeele, P., and Van de Wiele, T. (2015). Improved *in vitro* assay for determining the mucin adherence of bacteria sensitive to Triton X-100 treatment. *Folia Microbiol.* 60, 435–442. doi: 10.1007/s12223-015-0376-0
- Wali, M. K., and Abed, M. M. (2019). Antibacterial activity of acetic acid against different types of bacteria causes food spoilage. *J. Food Technol. Preserv.* 19, 1827–1831. Available online at: <https://www.alliedacademies.org/articles/antibacterial-activity-of-acetic-acid-against-different-types-of-bacteria-causes-food-spoilage-11256.html>
- Westerik, N., Kort, R., Sybesma, W., and Reid, G. (2018). *Lactobacillus rhamnosus* probiotic food as a tool for empowerment across the value chain in Africa. *Front. Microbiol.* 9, 1501. doi: 10.3389/fmicb.2018.01501
- Yukioka, Y., Tanahashi, T., Shida, K., Oguchi, H., Ogawa, S., Saito, C., et al. (2017). A role of nitrite reductase (NirBD) for NO homeostatic regulation in *Streptomyces coelicolor* A3. *FEMS Microbiol. Lett.* 364, 241. doi: 10.1093/femsle/fnw241
- Zhao, X. W., Zhou, M. H., Li, Q. B., Lu, Y. H., He, N., Sun, D. H., et al. (2005). Simultaneous mercury bioaccumulation and cell propagation by genetically engineered *Escherichia coli*. *Process Biochem.* 40, 1611–1616. doi: 10.1016/j.procbio.2004.06.014
- Zokaefar, H., Babaei, N., Saad, C. R., Kamarudin, M. S., Sijam, K., and Balcazar, J. L. (2014). Administration of *Bacillus subtilis* strains in the rearing water enhances the water quality, growth performance, immune response, and resistance against *Vibrio harveyi* infection in juvenile white shrimp, *Litopenaeus vannamei*. *Fish Shellf. Immunol.* 36, 68–74. doi: 10.1016/j.fsi.2013.10.007